ELSEVIER

A titania thin film annular photocatalytic reactor for the degradation of polycyclic aromatic hydrocarbons in dilute water streams

Hong Fei Lin, Kalliat T. Valsaraj*

Gordon A and Mary Cain Department of Chemical Engineering, Louisiana State University, Baton Rouge, LA 70803-7303, USA

Abstract

An external lamp, annular photocatalytic reactor with titania immobilized on a quartz tube was used to degrade two polycyclic aromatic hydrocarbons (PAHs), viz. phenanthrene (PHE) and pyrene (PYR) from a dilute water stream. The thin film geometry was used to obtain both the mass transfer coefficients and intrinsic reaction rate constants for the two compounds on immobilized titania (Degussa P-25) particles. Beyond a feed velocity of $7 \, cm \, min^{-1}$, the conversion was solely reaction rate controlled and was not subjected to mass transfer limitations from the aqueous phase to the immobilized titania film. The overall reaction rate constant was independent of the feed concentration as large as the saturation aqueous solubility of the two compounds. However, the conversion was dependant on the ultraviolet (UV) light illumination intensity at the reactor. The quantum efficiency ranged from 3.7×10^{-5} to 2.7×10^{-4} which was somewhat low because of the very low aqueous concentrations of the chemicals. The overall reaction rate constant was 1.6 times larger for pyrene than for phenanthrene. Seven reaction intermediates were identified for the conversion of phenanthrene, while for the degradation of pyrene two intermediates were identified. The presence of the phthalate ester as an intermediate product in the degradation of both PAHs indicates the presence of a quinone in both cases which degrades to the products CO_2 and H_2O, along with other stable intermediates. Mass balance in a batch reactor showed that only 28.6–40.1% of phenanthrene is mineralized to CO_2 in 1–3 h of reaction although 35–67% of the parent compound has disappeared, confirming that a substantial fraction of the parent compound has been converted to stable intermediates that remain in the reactor. A plausible mechanism based on these observations is proposed.
© 2003 Elsevier Science B.V. All rights reserved.

Keywords: Photocatalysis; Polycyclic aromatic hydrocarbons; Titania thin film; Annular reactor; Reaction mechanisms

---

*Corresponding author. Tel.: +1-225-578-6522; fax: +1-225-578-1476.
E-mail address: valsaraj@che.lsu.edu (K.T. Valsaraj).

1. Introduction

A recent workshop on industrial chemical separation needs identified "dilute solution" separations as a major focus for research [1]. Solutions that have <3 mol% organic contaminants are classified as dilute, but constitute a very large volume of industrial wastewater. Organic contaminants are mainly chlorinated compounds and hydrocarbons. Many of the traditional unit operations such as distillation, solvent extraction, stripping, adsorption, and absorption are either infeasible or uneconomical for dilute solutions. Remediation technologies such as incineration, biodegradation, and steam stripping are also uneconomical because the compounds are toxic and/or require treatment of very large volumes of water. Catalytic oxidation technologies using chemical or photochemical agents are more appropriate for treatment and destruction of contaminants at dilute concentrations.

The abundance of solar energy makes the use of ultraviolet (UV) detoxification of industrial wastewater an attractive technology [2]. Heterogeneous photocatalysis using semiconductors (for example, titanium dioxide (TiO_2)) is a well-studied process in this regard. Although extremely successful in the laboratory and moderately so on pilot scale, there are yet a number of factors that limit its utilization on the industrial scale. These factors include: (a) loss of photoactivity and surface area upon immobilization of a photocatalyst on inert supports; (b) reduced mass transfer in large reactors; (c) inefficient UV light energy utilization; (d) catalyst poisoning; and (e) low wastewater throughput in the reactor [3].

Our work in this field is directed primarily towards understanding the above factors and designing more efficient photochemical reactors [4,5]. Based on an exhaustive review of the literature and on model simulations, we concluded that a monolithic reactor configuration would afford the optimum mass transfer rates and reactor throughput [5]. A ceramic monolithic reactor with titania coating that uses optical fibers for UV light delivery is the current focus of study in our laboratory.

Optical fibers have quartz as the backbone material. In the monolithic reactor, titania is immobilized on the optical fibers and the ceramic monolith. Recent work by Pilkerton et al. [6] showed that the ability to irradiate the interior of a catalyst coated on an optical microfiber resulted in a faster rate of photodecomposition of ethanol than those for monolayer titania catalyst supported on porous vicor glass. Prior to detailed design, we need information on the mass transfer and photoreaction rate constants for compounds on titania film within the reactor. The present work was undertaken in response to the above need.

There are two classes of compounds that we are interested in our laboratory, viz. chlorinated benzenes and polycyclic aromatic hydrocarbons (PAHs). Our previous paper dealt with the degradation of a chlorinated aromatic compound, 1,2-dichlorobenzene, using titania on quartz tube [5]. We observed that complete mineralization of dichlorobenzene was possible at moderate UV illumination with titania as the photocatalyst. PAHs are the compounds of concern in the present work. PAHs form a class of refractory pollutants that are persistent in air, water and soil/sediment environments. They are produced as a result of fossil fuel energy usage, although some are of natural origin as well. Typically, most PAHs have small aqueous solubility and low vapor pressure. As a result, they are hydrophobic and accumulate in organic-rich environments such as soils, sediments and lipids in biota. Large molecular weight PAHs are toxic and difficult to treat in wastewaters. Photocatalytic

degradation is a likely pathway for removal as reported in two recent papers [7,8]. Apart from the two referenced papers there is no other literature that detail the semiconductor titania-mediated photocatalysis of PAHs in water. The reports only describe completely mixed batch reactor data that are not particularly useful for scale-up of a continuous reactor. The present paper, therefore, explores laboratory data in a continuous annular thin film reactor to elucidate mass transfer effects, and identify possible intermediates in the photodegradation process.
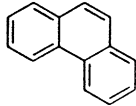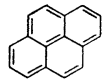
2. Experimental

2.1. Materials

Semiconductor titania was supplied by Degussa Corporation, Akron, PA. It had a surface area of 60–70 $m^2 g^{-1}$, mean particle diameter of 20 nm, and a zero point of charge with pH of 6.8.

Two polycyclic aromatic hydrocarbons were considered, namely, phenanthrene (PHE, 98% pure) and pyrene (PYR, 98% pure), both obtained from Aldrich. PHE is a three-ring compound, whereas PYR is a four-ring compound. Both compounds have low aqueous solubility and vapor pressure, and are extremely hydrophobic as evidenced by their octanol–water partition coefficients. Table 1 lists the relevant properties. Feed solutions of PHE and PYR were prepared by dissolving a known amount of the pure compound in distilled water.

2.2. Continuous reactor

Fig. 1 is the schematic of the photoreactor and ancillaries used in this work. A cylindrical glass reactor (38.2 cm long and 0.6 cm i.d.) was fabricated and a quartz rod (38 cm long and 0.3 cm i.d.) was inserted and fixed into the center of the reactor. The solution was pumped through the annular space within the reactor using an external pump at flow rates from 0.5

Table 1
Physicochemical properties of the PAHs

Property	Phenanthrene	Pyrene
Structure		
Molecular weight	178.24	202.26
Aqueous solubility (mg l^{-1})	1	0.15
Vapor pressure (mmHg)	2.5×10^{-4}	4.5×10^{-5}
log K_{aw}	−2.6	−3.3
log K_{ow}	4.5	5.1

Note: K_{aw} is the dimensionless air–water partition constant (molar concentration ratio) and K_{ow} the dimensionless octanol–water partition constant (molar concentration ratio). The latter parameter is a measure of the activity coefficient (hydrophobicity) of the compound in water. All values are at 25 °C.
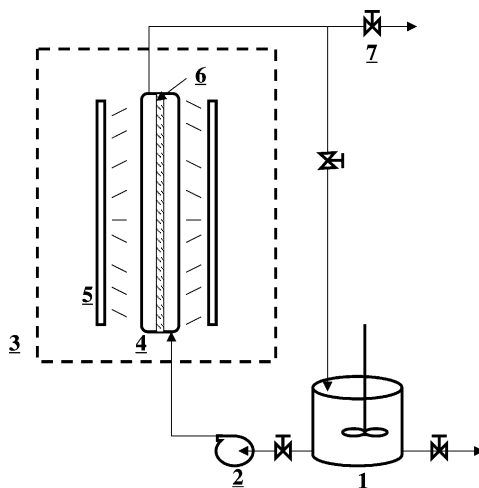
Fig. 1. Schematic of the semi-batch annular photocatalytic reactor used in the experiments: (1) PAH aqueous feed reservoir; (2) pump; (3) constant temperature chamber; (4) annular quartz reactor; (5) UV lamps; (6) inner quartz rod with thin film of titania; and (7) exit valve.

to 3.5 ml min^{-1}. The outer surface of the quartz rod was coated with a thin film of TiO$_2$ at a surface density of 0.007 g cm^{-2} using a dip-coat immobilization technique described earlier [5]. The surface density value was chosen based on our earlier work [5]. Four UV lamps (UVP Inc., Upland, CA) were placed around the reactor to give UV light intensity of 1–8 mW cm^{-2} at the reactor depending on the distance from the reactor. The incident light flux at the reactor was measured using a UVX radiometer obtained from UVP Inc. The entire reactor was kept in a chamber where the temperature was controlled to 40 ± 2 °C.

The reactor was configured for both single and multiple pass continuous modes of operation (Fig. 2). For the multiple pass experiments, the exit stream was mixed with the feed and continuously recycled. For the single pass experiment, the exit stream was collected in a separate container. Periodic samples were obtained from the inlet and exit in both cases. Feed solution containing PAHs at desired concentrations were fed to the reactor at the bottom using a pump at various flow rates up to 3.5 ml min^{-1}. The feed solution was prepared by diluting a saturated solution of the target PAH in distilled water.

To start the experiment, the feed solution of known pH was circulated through the reactor without UV light for approximately 1 h so that the inlet and outlet concentrations remained same indicating that steady state adsorption and a constant surface charge on titania was achieved. The UV light was then switched on and the feed and exit concentrations were monitored to obtain the conversion in the reactor. This was continued till steady state conversion was achieved under the given flow conditions.

2.3. Batch reactor

A few experiments were also conducted in the batch reactor with titania in the suspension mode as we described in our earlier work [5]. Phenanthrene (0.0838 g) was first deposited
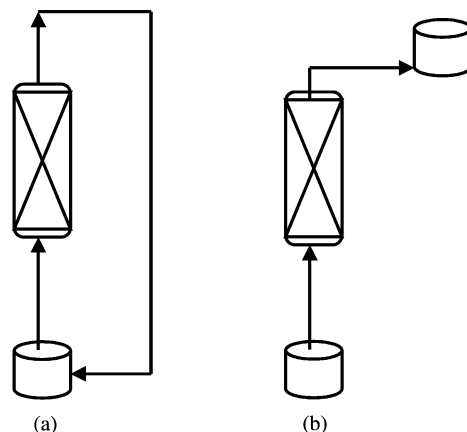
Fig. 2. Schematic of the reactor configuration: (a) multiple pass with feed recycle; and (b) single pass without feed recycle.

onto 2.128 g of titania from an ether solution of phenanthrene. The solution was stirred in the dark for adsorption equilibrium. It was air-dried in the dark to remove ether. Two hundred milligrams of titania with adsorbed phenanthrene mixture was suspended in 100 ml of aqueous solution, stirred for 30 min in the dark and was subjected to UV irradiation at 8.1 mW cm^{-2} for 1 and 3 h duration. A blank experiment was also conducted without UV light irradiation to compensate for the experimental errors and determine the initial mass of phenanthrene adsorbed onto titania. The solution in the batch reactor was continuously purged with pure air at a constant flow rate and the carbon dioxide formed was collected by passing through two bottles of saturated barium hydroxide (200 ml each). The titania solution was filtered after reaction using a Millipore filter and the filtrate transferred to a separatory funnel. The titania was then rinsed with 20 ml chloroform to extract the residual phenanthrene on the surface. The aqueous filtrate was also extracted using chloroform. The two extracts were combined and blown down by soft nitrogen flow to 2 ml. The sample was then used for GC–MS analysis. The barium hydroxide from the bottles was filtered, baked in an oven and weighed to obtain the barium carbonate weight from which the amount of CO$_2$ collected was determined.

2.4. Analysis of PAHs

PHE and PYR in the exit and feed streams were determined by direct injection into a Hewlett-Packard liquid chromatograph (HP 1100) equipped with a UV-Vis diode array detector. The aqueous solution was directly injected into the HPLC. The column used was Phenomenex Envirosep-PP (125 mm × 3.2 mm). The parameters and HPLC conditions used for the analysis were that for the US EPA Standard Method No. 8270 [12]. GC–MS analysis was conducted using an HP 5890 GC–MS coupled to a mass selective detector (HP 5973) and compound identification was done using an NBS mass spectral library. The GC column was J&W Scientific DB-5 (30 m × 0.25 mm).

The intermediates were analyzed using a HP 5890 GC–MS with a mass selective detector (HP 5971). A glass capillary column (30 m long, 0.25 mm i.d.) coated with DB-5 was obtained from Phenomenex. The oven temperature was held for 1 min at 45 °C and temperature ramped at 30 °C min^{-1} to 130 °C which was held for 3 min and another temperature ramp of 12 °C min^{-1} to a final temperature of 325 °C. The injector temperature was 300 °C and the detector temperature was 325 °C. The carrier gas was helium at 0.571 ml min^{-1}. Compound identification was done using the NBS mass spectral library.

3. Results and discussion

3.1. Analysis of reactor data

The steady state efficiency (conversion) in the thin film continuous annular reactor was obtained from the experimental data as:

$$x = 1 - \frac{C(L)}{C_0} \tag{1}$$

where $C(L)$ is the exit concentration in a reactor of length L (cm), and C_0 the feed concentration at the inlet.

The conversion in the reactor was used to obtain the overall reaction rate constant [5]:

$$k^* = -\frac{u}{L} \ln (1 - x) \tag{2}$$

where u is the superficial liquid velocity (cm min^{-1}). The overall rate constant derives two contributions, a mass transfer rate from the liquid phase to titania and an intrinsic reaction rate [5,8]:

$$\frac{1}{k^*} = \frac{1}{kK} + \frac{1}{k_m a_v} \tag{3}$$

where k is the surface reaction rate constant (mol l^{-1} min^{-1}), K the Langmuir–Hinshelwood adsorption constant (l mol^{-1}), k_m the mass transfer coefficient (cm min^{-1}), and a_v the surface area of titania per unit volume of the reactor (cm^2 cm^{-3}).

As mentioned earlier (see also Fig. 2), the process was conducted in both single and multiple pass modes. In the single pass mode, the feed concentration was maintained constant and the exit stream was not recirculated. In the multiple pass mode, the exit stream was recirculated through the reactor after mixing with the feed in the reservoir. In the multiple pass mode, both the feed and exit streams declined in concentrations with time. Fig. 3a and b show the PHE concentration in the exit and inlet streams for the two cases for a given feed velocity of 7.26 cm min^{-1}. The steady state removals are also shown in the figure. The time shown on the x-axis for the multiple pass experiment reflects the number of passes in the plug-flow reactor. Using an average residence time of 5.2 min, one can estimate that at 400 min, the number of passes is 77. The overall removal per pass remained steady and the process is, therefore, at quasi-steady state. Note that the steady state removals remained a constant in both cases. As a result, the observed rate constant k^* was also similar in both
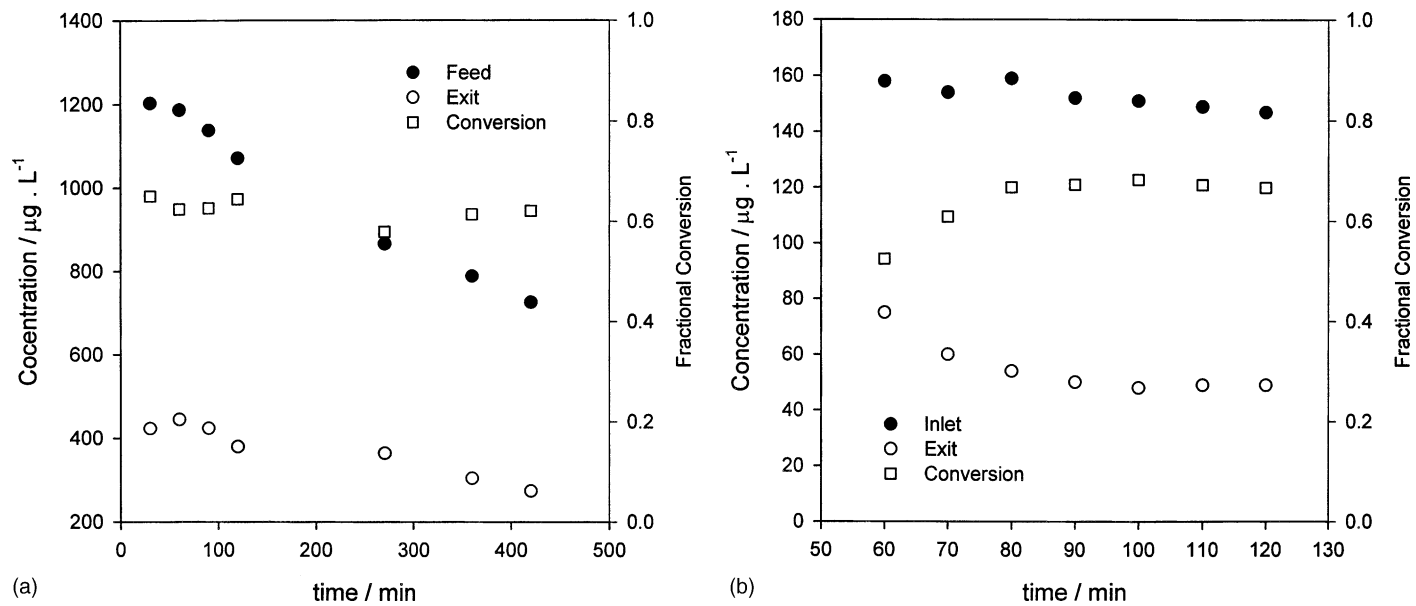
Fig. 3. Feed and exit concentrations of phenanthrene and the conversion in the reactor as a function of time for: (a) multiple pass with feed recycle; and (b) single pass without feed recycle.
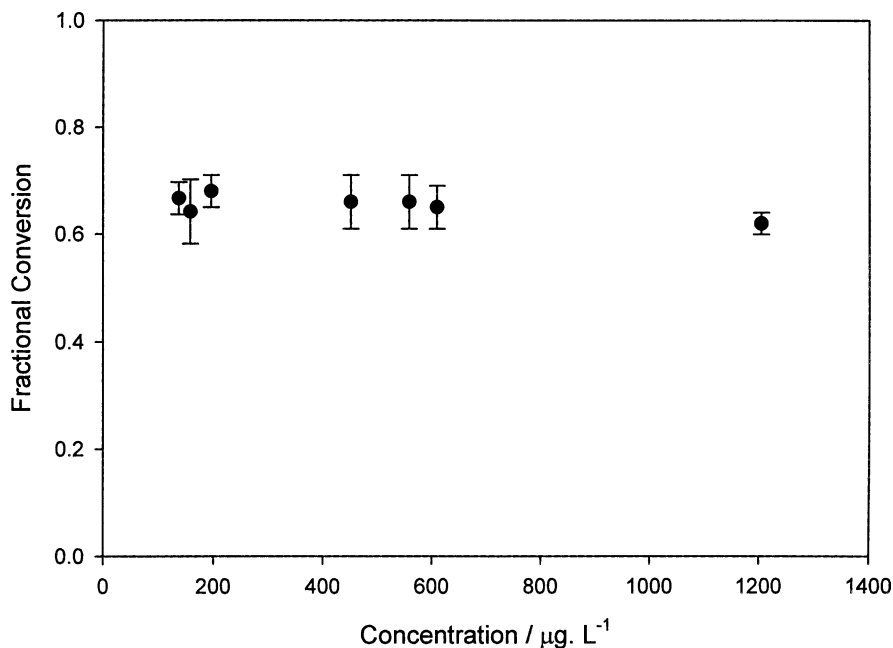
Fig. 4. Fractional conversion of phenanthrene in the reactor as a function of initial feed concentration.

cases. Therefore, we conclude that both modes of operation are equivalent in extracting reaction rate parameters for PAHs.

3.2. Effects of feed concentration

The effect of PHE concentration upon fractional conversion was studied for the range between 100 and 1200 $\mu g\,l^{-1}$. This is shown in Fig. 4 for a feed velocity of 7.26 cm min^{-1}. It was observed that the fractional conversion did not show any discernible difference or trend in the range of concentrations investigated. Noting that the maximum concentration used was the aqueous solubility of PHE, and that the photodegradation of PHE is not a function of the concentration, it is clear that the adsorption on titania is in the linear region of the Langmuir adsorption isotherm. Only under these circumstances, Eqs. (2) and (3) will be valid. This also underscores the fact that the linear isotherm assumption for PHE on titania is valid at concentrations as large as the saturation solubility of PAHs. In other words, the saturation adsorption capacity for PAHs on titania is never reached. Recent adsorption studies of PHE on titania and alumina also corroborate this conclusion [8,10].

The quantum yield for the photooxidation was obtained from:

$$\phi = \frac{k^*C}{\mathrm{d}[h\nu]/\mathrm{d}t}$$

where $\mathrm{d}[h\nu]/\mathrm{d}t$ is the incident photon flux per unit volume. The incident photon flux was $1.6 \times 10^{-6}\,\mathrm{mol\,s^{-1}}$ at the reactor obtained from the measured UV intensity of 8 mW cm^{-2}.

The quantum yield obtained varied from 3.7×10^{-5} to 2.7×10^{-4} for PHE at aqueous concentrations varying from 0.77 to 6.7 μM. The low values are attributable to the low PHE concentrations in water. Since oxidation processes involve secondary reactions between primary radicals (hydroxyl and superoxide) and substrates, the quantum yield will depend on substrate concentration.

3.3. Effects of feed velocity

The effect of the liquid feed velocity on the rate constant is shown in Fig. 5. Fig. 5a shows the variation in k^* at flow velocities ranging from 0.5 to 15 cm min^{-1}. Both PHE and PYR showed similar trends. The value of the overall rate constant appears to be independent of u at values greater than 7 cm min^{-1}, while it shows a linear dependence at smaller flow velocities. Notice, however, that the conversion x decreased as u increased (Fig. 5b). For a given reactor length, increasing u decreases the residence time, and hence the overall conversion of PHE and PYR decrease. However, since k^* is logarithmically related to x (Eq. (2)), increased velocity increased k^* as shown in Fig. 5a. There is a specific reason for the dependence of rate constant on u. For this we turn to Eq. (3) which represents the magnitude of mass transfer and intrinsic reaction terms on the overall rate constant. Eq. (3) shows that the overall resistance to conversion ($1/k^*$) is the sum of the mass transfer resistance ($1/k_m a_v$) and that due to intrinsic reaction ($1/kK$). The intrinsic reaction term is independent of u while the mass transfer resistance decreases as u increases [5,9,11]. k_m represents the mass transfer of the compound from the aqueous phase to the catalyst surface through the aqueous boundary layer; this is called the diffusion limited or mass transfer controlled regime. Increasing u decreases the boundary layer resistance in the liquid phase, and consequently decreases the term $1/k_m a_v$, and increases the overall rate constant k^*. Once the mass transfer limitation is overcome at high u, the conversion is limited only by the intrinsic reaction rate which is independent of u. Thus, at high flow rates (>7 cm min^{-1}) we reach the reaction limited region. The delineation of this region is of importance in designing our photocatalytic monolithic reactor using immobilized catalysts.

An important observation from Fig. 5a is that the intrinsic reaction rate constant ($k^* = kK$ at $u > 7$ cm min^{-1}) for PYR is 1.6 times larger than that for PHE under similar conditions of flow and UV illumination intensity (Table 2). This difference is primarily a result of the higher adsorption constant K for PYR than for PHE due to the much larger hydrophobic nature of PYR. This is evident from the fact that logarithm of the octanol–water partition constant is 4.57 for PHE as opposed to 5.13 for PYR (Table 1). In Table 2, we also list the photolysis rate constants for the two PAHs in pure water as it occurs under UV illumination. As noted, these rate constants are much lower than the titania-catalyzed process.

3.4. Effects of UV light intensity

The UV light intensity at the reactor was varied by changing the distance of the UV lamps from the reactor. The radiant flux corresponds to approximately 20% of the total electrical power consumed in the reaction. Fig. 6 shows that the reaction rate constant increased linearly with the UV illumination intensity up to ≈ 2 mW cm^{-2} and thereafter
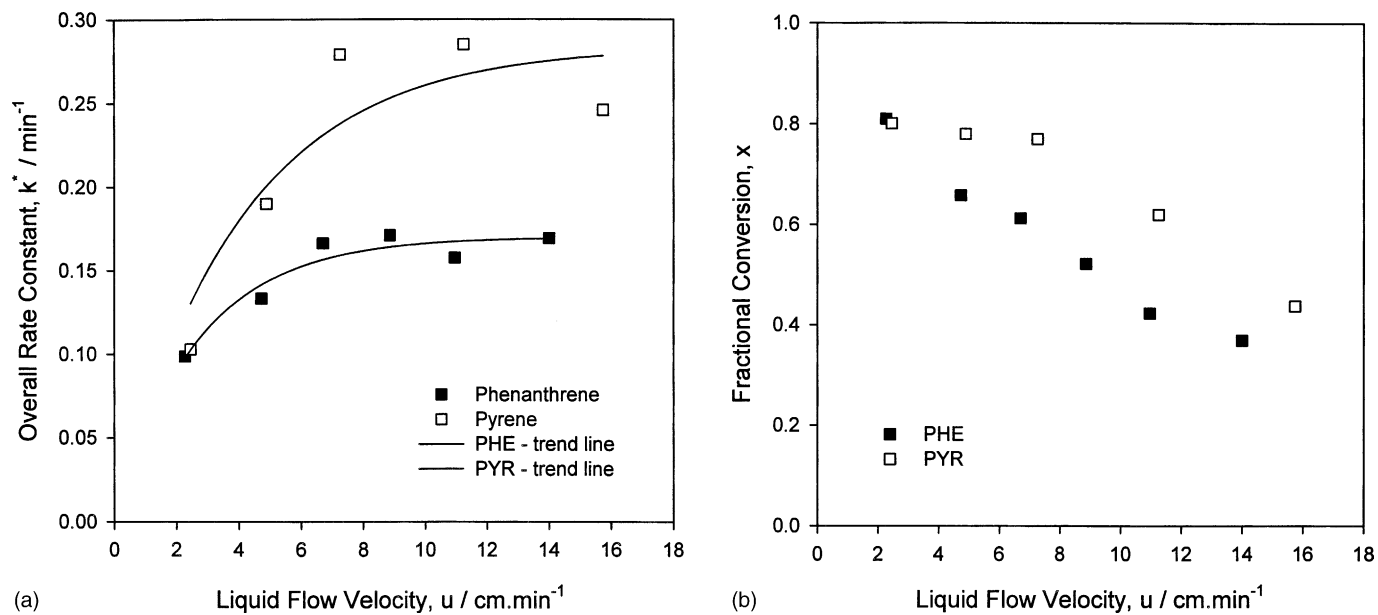
Fig. 5. Overall rate constants (a) and fractional conversions (b) for phenanthrene and pyrene in the reactor as a function of feed velocity.

Table 2
Reaction rate constant and half life for PAHs with and without titania catalyst

Parameter	Phenanthrene	Pyrene
Thin film titania catalyzed[a]		
Intrinsic reaction rate constant (min^{-1})	0.166 ± 0.006	0.270 ± 0.021
Half life (min)	4.2 ± 0.2	2.6 ± 0.2
Aqueous photolysis (without titania catalyst)[b]		
Reaction rate constant (min^{-1})	5.4×10^{-4}	0.0234
Half life (min)	1283	29

[a] These values are applicable for the reactor geometry that we have used and valid for the reaction rate controlled regime, where $u > 7\,cm\,min^{-1}$.

[b] The photolysis of PAHs were conducted in pure water in the presence of oxygen at wavelengths >290 nm [15].

showed smaller changes up to $8\,mW\,cm^{-2}$. It is generally known that above a certain UV photon flux, the reaction rate dependency goes from first order in the reactant concentration to a one-half order; the transition occurring at different intensities for different compounds and reactor configurations [2]. From our results we conclude that an optimum UV intensity of $2\,mW\,cm^{-2}$ is required for our reactor configuration.
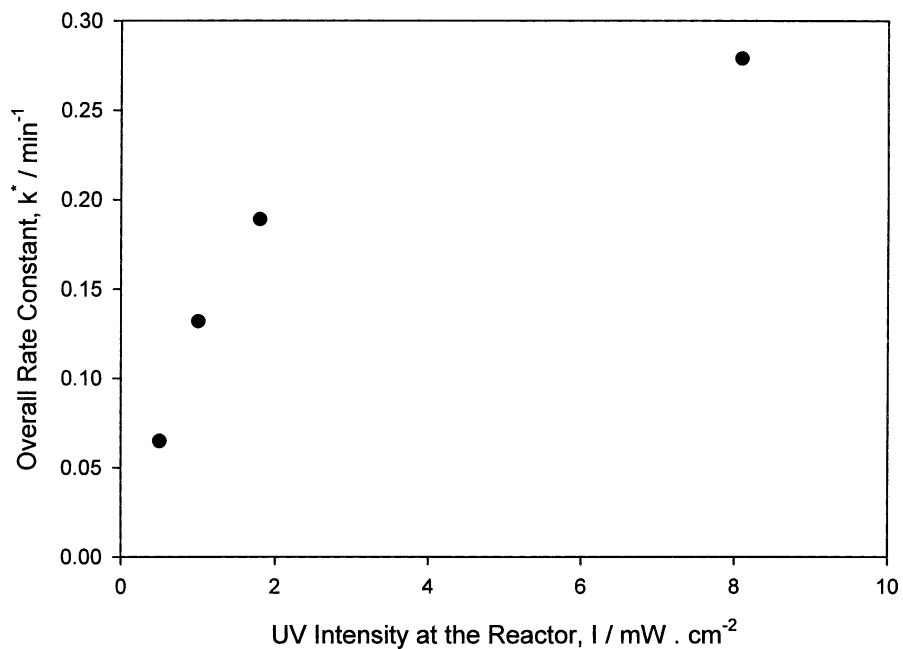

Fig. 6. Overall rate constant for the conversion of phenanthrene as a function of the UV light intensity at the reactor.

3.5. Analysis of reaction products and intermediates

Although photooxidation is an efficient process for conversion of PAHs, it is instructive to remember that the focus should not only be on the disappearance of the parent compound but also on the intermediates that may be produced during the catalysis. It is important to make sure that the intermediates formed are not of higher toxicity than the parent compound. As a result, we conducted extensive analysis of the aqueous solutions during the reaction using both GC–MS and HPLC.

HPLC and GC–MS analysis of the aqueous samples showed that 9,10-phenanthrenequinone was an intermediate in the degradation of phenanthrene. It is also a known intermediate in the conventional direct UV photolysis of phenanthrene in natural water as described by various other investigators [13]. The e^-/h^+ couple generated by UV ($<410\,nm$) illumination of titania will generate highly oxidizing species as per the following sequence of reactions:

$$TiO_2 + h\nu \rightarrow e^- + h^+$$
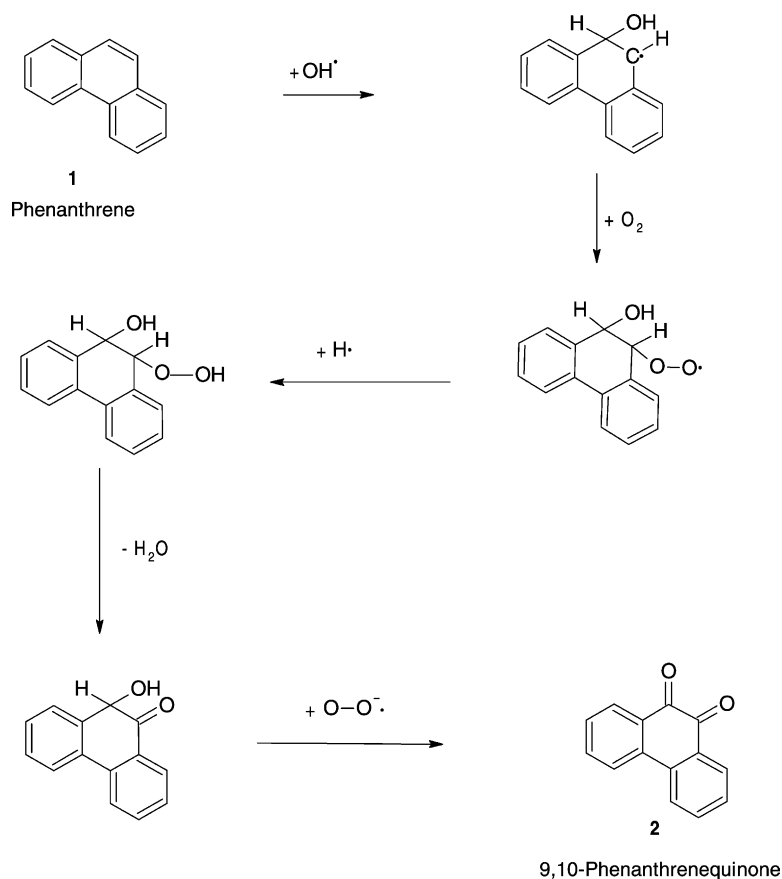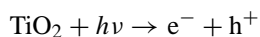
Scheme 1. The postulated mechanism of the conversion of phenanthrene to 9,10-phenanthrenequinone.

t=21.83mins   1,2-Benzenedicarboxylic acid, mono(2-ethylhexyl) ester; (**3**)
t=21.74mins   1,2-benzenedicarboxylic acid, diisooctyl ester (**4**)
t=19.75mins   9,10-Phenanthrenedione, (**2**)
t=19.30mins   2-Phenanthrenol, (**6**)
t=18.93mins   9,10-Dihydro-9,10-dihydroxyphenanthrene
t=17.64mins   Phenanthrene, 2-methyl-, (**5**)
t=16.99mins   (1,1'-Biphenyl)-2,2'-dicarboxaldehyde, (**9**)
t=16.43mins   Phenanthrene, (**1**)
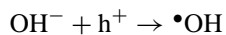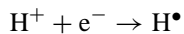t=15.53mins   9H-Fluorene, 4-methyl-, (**8**)
t=14.24mins   Fluorene, (**7**)

Fig. 7. GC–MS trace of the solution after 60 min of reaction in the batch mode.

$$H_2O \rightarrow H^+ + OH^-$$

$$H^+ + e^- \rightarrow H^\bullet$$

$$OH^- + h^+ \rightarrow {}^\bullet OH$$

$$O_2 + e^- \rightarrow O_2{}^{\bullet -}$$
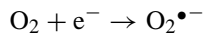
Hydroxyl ($^\bullet OH$) and superoxide ($O_2{}^{\bullet -}$) radicals are the primary oxidizing species in heterogeneous photocatalytic processes. The resulting hydroxyl radical attack on the 9-position
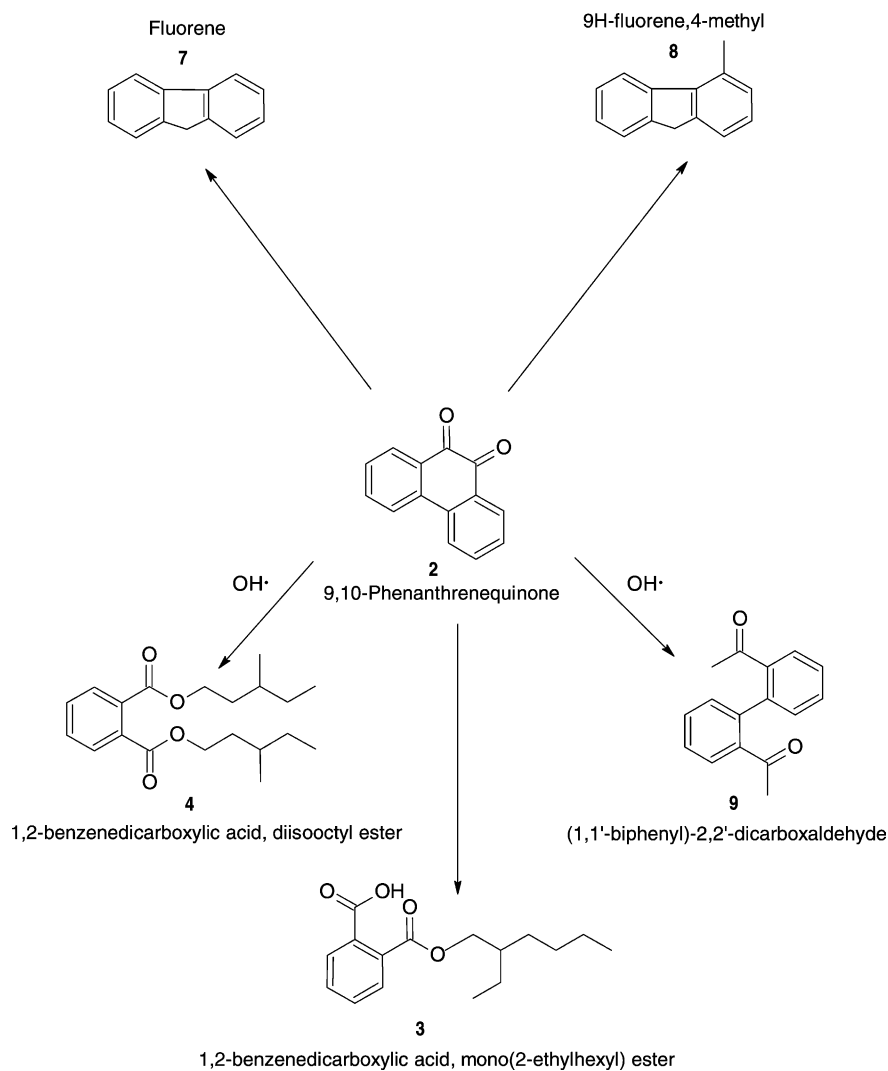
Scheme 2. The various intermediates that result from 9,10-phenanthrenequinone identified by GC–MS.

of **1** (phenanthrene) and subsequent reaction with oxygen and superoxide radical will lead to the formation of **2** (9,10-phenanthrenequinone). The plausible mechanism is shown in Scheme 1. GC–MS peak area for this compound was very small in the early stages of the reaction and was non-existent in the later samples. This indicates that **2** is a transient species and is probably easily oxidized to other species. Matsuzawa [14] has shown that **2** undergoes photolysis by UV light to produce phthalic acid. Fig. 7 shows the GC–MS trace of the aqueous solution containing phenanthrene and titania after 60 min of treatment in the batch reactor. Seven intermediates (**3**–**9**) were isolated and identified in the GC–MS trace for phenanthrene degradation. It is proposed that **2** undergoes ring opening and subsequent reaction with the alkyl radicals generated by TiO_2 photooxidation to form the various intermediates **3**, **4**, and **9** (Scheme 2). The other intermediates **7** and **8** are believed to be formed by further hydroxyl radical attack on **9**. Compounds **5** and **6** are formed by direct addition of $^\bullet OH$ or $^\bullet CH_3$ radicals to the parent compound **1** and further elimination/rearrangement in some cases (Scheme 3). Aldehydes and esters have also been observed in the conventional photolytic oxidation (UV or ozone) of PAHs [13]. For the
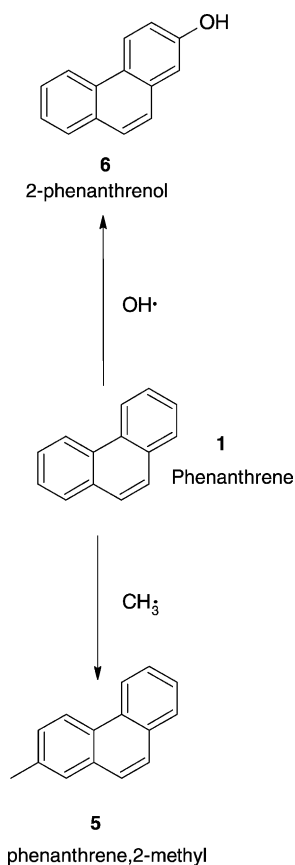
Scheme 3. Direct addition of hydroxyl and methyl radicals to phenanthrene.

Table 3
Mineralization of phenanthrene to carbon dioxide

Reaction time (h)	Percent phenanthrene removed	Moles of phenanthrene removed	Moles of CO_2 for complete mineralization of phenanthrene	Actual moles of CO_2 observed	Percent conversion to CO_2
1	35.1	9.108×10^{-6}	1.275×10^{-4}	3.469×10^{-5}	28.6
3	67.6	9.653×10^{-6}	1.352×10^{-4}	5.422×10^{-5}	40.1

photooxidation of **10** (pyrene), we observed two intermediates in the mass spectral analysis, viz. **11** (naphthalene-1,2,3,4-tetrahydro-1-phenyl) and **12** (bis(2-ethylhexyl)phthalate). The presence of **12** is once again indication of the formation of a quinone with a subsequent ring opening reaction.

The amount of CO_2 generated during the reaction is an indication of whether photocatalysis is capable of complete mineralization of phenanthrene to CO_2 and water. Batch experiment using phenanthrene was very useful in this regard. Table 3 displays the data from the mass balance in the batch reactor where the amounts of phenanthrene and CO_2 after 1 and 3 h of reaction were determined. The mass of phenanthrene removed is 35% in 1 h and 67% in 3 h of reaction. However, only 28.6% of the phenanthrene is converted to CO_2 in 1 h and 40.1% in 3 h of reaction. This is an indication that although a substantial portion of phenanthrene on the titania surface has reacted photochemically, a fraction of the phenanthrene is converted to stable products via radical recombination mechanisms. This indicates that with large reaction times in a reactor there is the distinct possibility of formation of stable intermediates which can be more toxic than the parent compound. This fact was also noted for the photodegradation of naphthalene on titania [7]. This is a limitation of the heterogeneous photochemical degradation of polycyclic aromatic hydrocarbons.

Acknowledgements

References

[1] Roadmap on Chemical Separations, American Institute of Chemical Engineers, New York, NY, 2000.
[2] J.B. Galvez, S.M. Rodriguez, Solar Detoxification, Report to the UNESCO Program on Energy, Wiley–UNESCO Energy Engineering Learning Package, Cedex France, 2001.
[3] A.K. Ray, Chem. Eng. Sci. 54 (1999) 3113–3125.
[4] Q. Yuan, R. Ravikrishna, K.T. Valsaraj, Sep. Purif. Technol. 24 (2001) 309–318.
[5] H.F. Lin, R. Ravikrishna, K.T. Valsaraj, Sep. Purif. Technol. 28 (2002) 87–102.
[6] S. Pilkerton, S.-J. Hwang, D. Raftery, J. Phys. Chem. B 103 (1999) 11152–11160.
[7] S. Das, M. Muneer, K.R. Gopidas, J. Photochem. Photobiol. A: Chem. 77 (1994) 83–88.

[8] S. Wen, J. Zhao, G. Sheng, J. Fu, P. Peng, Chemosphere 46 (2002) 871–877.
[9] V. Balakotiah, N. Gupta, D.H. West, Chem. Eng. Sci. 55 (2000) 5367–5383.
[10] P.M. Jain, J.S. Smith, K.T. Valsaraj, Sep. Purif. Technol. 17 (1999) 21–30.
[11] C.F. Turchi, D.F. Ollis, J. Phys. Chem. 92 (1988) 6852–6853.
[12] US Environmental Protection Agency, Standard Methods for Analysis of Wastes and Wastewaters, Method No. 8270.
[13] Y. Zeng, A.P.K. Hong, D.A. Wavrek, Water Res. 34 (2000) 1157.
[14] S. Matzuzawa, Polycyclic Aromat. Compd. 21 (2000) 331–339.
[15] M.P. Fasnacht, N.V. Blough, Environ. Sci. Technol. 36 (2002) 4364–4369.